Multivariate Curve Resolution Analysis for Interpretation of Dynamic Cu K-Edge X-ray Absorption Spectroscopy Spectra for a Cu Doped V2O5 Lithium Battery

ARTICLE *in* ANALYTICAL CHEMISTRY · MARCH 2010

Impact Factor: 5.64 · DOI: 10.1021/ac902865h · Source: PubMed

5 AUTHORS, INCLUDING:

Paolo Conti
University of Camerino
21 PUBLICATIONS **178** CITATIONS
SEE PROFILE

Marco Giorgetti
University of Bologna
85 PUBLICATIONS **1,270** CITATIONS
SEE PROFILE

Mario Berrettoni
University of Bologna
91 PUBLICATIONS **1,766** CITATIONS
SEE PROFILE

William H Smyrl
University of Minnesota Twin Cities
252 PUBLICATIONS **5,200** CITATIONS
SEE PROFILE

Anal. Chem. **2010,** *82,* 3629–3635

Multivariate Curve Resolution Analysis for Interpretation of Dynamic Cu K-Edge X-ray Absorption Spectroscopy Spectra for a Cu Doped V_2O_5 Lithium Battery

Paolo Conti and Silvia Zamponi

Dipartimento di Chimica, Università di Camerino, 62032 Camerino (MC), Italy

Marco Giorgetti* and Mario Berrettoni

Department of Physical and Inorganic Chemistry, University of Bologna and Unità di Ricerca INSTM di Bologna, Viale del Risorgimento 4, 40136 Bologna, Italy

William H. Smyrl

Department of Chemical Engineering and Materials Science, University of Minnesota, 421 Washington Avenue South East, Minneapolis, Minnesota 55455

Vanadium pentoxide materials prepared through sol−gel processes act as excellent intercalation hosts for lithium as well as polyvalent cations. A chemometric approach has been applied to study the X-ray absorption near-edge structure (XANES) evolution during in situ scanning of the $Cu_{0.1}V_2O_5$ xerogel/Li ions battery. Among the more common techniques, the fixed size windows evolving factor analysis (FSWEFA) permits the number of species involved in the experiment to be determined and the range of existence of each of them. This result, combined with the constraints of the invariance of the total concentration and non-negativity of both concentrations and spectra, enabled us to obtain the spectra of the pure components using a multivariate curve resolution refined by an alternate least squares fitting procedure. This allowed the normalized concentration profile to be understood. This data treatment evidenced the occurrence, for the first time, of three species during the battery charging. This fact finds confirmation by comparison of the pure spectra with the experimental ones. Extended X-ray absorption fine structure (EXAFS) analysis confirms the occurrence of three different chemical environments of Cu during battery charging.

Vanadium pentoxide prepared via sol−gel processes has attracted much interest due to the facile and reversible intercalation of alkali ions into their lattices to form electrically conducting materials. The insertion reactions take place with a large free energy of formation, thus allowing applications as intercalation hosts for lithium ions, and some comprehensive reviews are available.[1−3] Previous studies by the X-ray absorption spectroscopy (XAS) technique on the V_2O_5 based compounds allowed us to determine fundamental structural information on a wide variety of native and pillared nanocomposites[4−11] using both ex situ and in situ (dynamic XAS) techniques. The dynamic XAS technique has enabled the identification of the chemical species involved in the charge−discharge process and to check for the structural and electronic reversibility of the materials upon lithium insertion. However, the extended X-ray absorption fine structure (EXAFS) analysis, which carries the structural information, is likely to be done on the fully discharged and fully charged cathode only, i.e., where the electrode composition was exclusively one single chemical phase. For instance, an in situ XAS experiment[10] showed that the copper ion, in the copper doped V_2O_5 cathode, was reduced to the metallic state during lithium insertion. Here, because we are interested in an in depth comprehension of

* To whom correspondence should be addressed. E-mail: marco.giorgetti@unibo.it. Phone: +39 051 209 3666. Fax: +39 051 209 3690.

(1) Chernova, N. A.; Roppolo, M.; Dillon, A. C.; Whittingham, M. S. *J. Mater. Chem.* **2009**, *19*, 2526.
(2) Livage, J. *Coord. Chem. Rev.* **1998**, *178−180*, 999.
(3) Chirayil, T.; Zavalij, P. Y.; Whittingham, M. S. *Chem. Mater.* **1998**, *10*, 2629.
(4) Giorgetti, M.; Passerini, S.; Smyrl, W. H.; Berrettoni, M. *Inorg. Chem.* **2000**, *39*, 1514.
(5) Giorgetti, M.; Passerini, S.; Smyrl, W. H.; Berrettoni, M. *Chem. Mater.* **1999**, *11*, 2257.
(6) Frabetti, E.; Deluga, G. A.; Smyrl, W. H.; Giorgetti, M.; Berrettoni, M. *J. Phys. Chem. B* **2004**, *108*, 3765.
(7) Giorgetti, M.; Passerini, S.; Berrettoni, M.; Smyrl, W. H. *J. Synchrotron Radiat.* **1999**, *6*, 743.
(8) Giorgetti, M.; Berrettoni, M.; Passerini, S.; Smyrl, W. H. *Electrochim. Acta* **2002**, *47*, 3163.
(9) Giorgetti, M.; Ascone, I.; Berrettoni, M.; Conti, P.; Zamponi, S.; Marassi, R. *J. Inorg. Biol. Chem.* **2000**, *5*, 156.
(10) Giorgetti, M.; Mukerjee, S.; Passerini, S.; Mc Breen, J.; Smyrl, W. H. *J. Electrochem. Soc.* **2001**, *148*, A768.
(11) Giorgetti, M.; Passerini, S.; Smyrl, W. H.; Mukerjee, S.; Yang, X. Q.; Mc Breen, J. *J. Electrochem. Soc.* **1999**, *146*, 2387.

10.1021/ac902865h
Published on Web 03/30/2010

the insertion chemistry of a cathodic material, we have used a joint XAS−chemometric approach.

In dynamic XAS, the matrix of the spectra is ordered on the basis of the elapsed time (potential): each row is a XAS spectrum at a fixed potential.[9−12] A similar matrix is useful to determine the number of chemical species in the sample sequence, as well as the concentration profile and the spectrum of each of them. Multivariate curve resolution (MCR) techniques,[13] the recent implementations of which are discussed by De Juan and Tauler,[14] permit to decompose the experimental matrix in a product of two matrixes to which can be attributed chemical meaning.[15] The factorization in multivariate curve resolution can be iteratively refined by alternating least squares (MCR-ALS).[16] A detailed theoretical description and some applications in spectroscopy are reviewed by Garrido et al.,[17] while Ni et al.[18] reported the impact of chemometric methods, in particular MCR-ALS, on the electroanalytical problems. To obtain a unique solution with physicochemical meaning by MCR-ALS, some constraints must be applied. These constraints are based on physicochemical features of the experiment, and they generally are the closure condition, non-negativity (of concentration and/or of pure response). Furthermore a tentative initial value, as close as possible to the final solution, of one of the matrixes have to be given to initialize the ALS refinement. For a long time, principal component analysis (PCA) and factor analysis (FA)[19] have been used to determine the rank of the matrix, generally assumed as the number of chemical species of the system, but PCA acts on the whole matrix returning its full rank. In the case of dynamic systems, we can apply a local PCA analysis to find the local rank of the data. Evolving factor analysis (EFA),[20,13] already used even in XAS analysis,[21,22] takes advantage of the ordered structure of the data matrix to point out the appearance and disappearance of each species. With this method, not only the number of species but also their evolution along the row index is assessed. Fixed size window EFA (FSWEFA)[23] was developed to test the peak purity in pharmaceutical chromatographic analysis and was found to be efficient in discovering low signal species disclosing their number in each window. These are two valuable methods to initialize the ALS refinement as both the number of species and the first tentative matrix can be received from them. With the combination of the initialization results from EFA or FSWEFA with the ALS refinement in MCR-ALS, a perfect description can be applied to both concentration profiles and absorption spectra.[24,25]

This article reports the study of the dynamic of the XANES spectra evolution during in situ scans of the $Cu_{0.1}V_2O_5$ xerogel/Li ions battery using the previous chemometric methods. The structures of the fully discharged and fully charged $Cu_{0.1}V_2O_5$ xerogel cathode are available in the literature.[10] It is indicated that the Cu ions are 4-fold coordinated by four oxygen in the native "just assembled" cell (before discharge) and that the lithium insertion in copper-doped V_2O_5 xerogel caused the reduction of copper to the metallic state. In addition, the process was completely reversible at the atomic level. No information on the number of species involved during the lithium insertion or release was extracted from the experiments.

Here, the chemometric analysis of the dynamic XANES spectra allows one to investigate in depth the entire lithiation process; FSWEFA analysis allows the number of phases during charging to be determined, and it is found more appropriate than EXAFS analysis only due to the large number of spectra taken throughout the battery charging.

EXPERIMENTAL SECTION

Synthesis and Electrode Preparation. Vanadium pentoxide hydrogels were synthesized by an ion exchange process with sodium metavanadate. The copper doped V_2O_5 was prepared, and characterized, as described in the literature[26] and references therein. Briefly, the doping was performed by mixing the selected stoichiometric amount of copper powder (ALFA 99.997% purity) with the V_2O_5 hydrogel. X-ray diffraction (XRD) spectra were taken on the dry, doped material in order to verify the completion of the reaction, i.e., if no peaks associated with metallic copper were found.

$Cu_{0.1}V_2O_5$ xerogel electrodes were prepared by spray coating a mixture of the active material with carbon (Ketjen black, Akzonobel) and binder (Kynar, ELF-Atochem) in cyclopentanone (Fluka), onto 25 μm thick aluminum foils. The final weight ratio of the three components in the dry cathode was 80:10:10, respectively. The active material mass loading ranged from 3 to 4 mg cm^{-2}.

XAS Experiments. To perform in situ XAS measurements, $Cu_{0.1}V_2O_5$ xerogel cathodes were placed in a special spectroelectrochemical cell. The in situ X-ray absorption experiments were performed at the National Synchrotron Light Source (NSLS) at Brookhaven National Laboratory using the beamline X11 A, operating at 2.5 GeV and a typical current of 310 mA. The details pertaining to the spectroelectrochemical cell, to the design of the monochromator, the resolution, and the detune procedure are available in the literature.[11,27] Internal references for energy calibration were used. Harmonics were rejected by detuning (50%). Data were acquired in fluorescence mode at the copper K-edge. XAS spectra were taken every 0.5 eV up to 50 eV after the edge with an integration time of 1 s and then collected up to $k = 13$ every $0.05k$ with a 3 s integration time.

XAS Data Analysis. XANES spectra were normalized to an edge jump of unity taking into account the atomic background

(12) Sharpe, L. R.; Heineman, W. R.; Elder, R. C. *Chem. Rev.* **1990**, *90*, 705.
(13) Vandeginste, B. G. M.; Massart, D. L.; Buydens, L. M. C.; De Jong, S.; Lewi, P. J.; Smeyers-Verbeke, J.; *Handbook of Chemometrics and Qualimetrics*, Part B; Elsevier: Amsterdam, The Netherlands, 1998.
(14) de Juan, A.; Tauler, R. *Crit. Rev. Anal. Chem.* **2006**, *36*, 163.
(15) de Juan, A.; Tauler, R. *Anal. Chim. Acta* **2003**, *500*, 195.
(16) Tauler, R. *Chemom. Intell. Lab. Syst.* **1995**, *30*, 133.
(17) Garrido, M.; Rius, F. X.; Larrechi, M. S. *Anal. Bioanal. Chem.* **2008**, *390*, 2059.
(18) Ni, Y.; Koko, S. *Anal. Chim. Acta* **2008**, *626*, 130.
(19) Brereton, R. G. *Chemometrics: Data Analysis for the Laboratory and Chemical Plants*; John Wiley & Sons: Chichester, U.K., 2003 (c'è sia PCA che EFA che FSWEFA).
(20) Maeder, M. *Anal. Chem.* **1987**, *59*, 527.
(21) Márquez-Alvarez, C.; Rodríguez-Ramos, I.; Guerrero-Ruiz, A.; Haller, G. L.; Fernández-García, M. *J. Am. Chem. Soc.* **1997**, *119*, 2905.
(22) Ciuparu, D.; Haider, P.; Fernández-García, M.; Chen, Y.; Lim, S.; Haller, G. L.; Pfefferle, L. *J. Phys. Chem. B* **2005**, *109*, 16332.
(23) Keller, H. R.; Massart, D. L. *Anal. Chim. Acta* **1991**, *246*, 379.
(24) Marassi, R.; Zamponi, S.; Conti, P.; Lanteri, S. *Ann. Chim.* **2002**, *92*, 261.
(25) Tomišić, V.; Simeon, V. *Phys. Chem. Chem. Phys.* **2000**, *2*, 1943.
(26) Giorgetti, M.; Berrettoni, M.; Smyrl, W. H. *Chem. Mater.* **2007**, *19*, 5991.
(27) Mc Breen, J.; Mukerjee, S. *J. Electrochem. Soc.* **1995**, *142*, 3399.

after the edge as revealed from the EXAFS analysis. A prior removal of the background absorption was done by subtraction of a linear function extrapolated from the pre-edge region. The EXAFS analysis has been performed by using the GNXAS package[28,29] that takes into account multiple scattering (MS) theory. The method is based on the decomposition of the EXAFS signals into a sum of several contributions, the *n*-body terms. It allows the direct comparison of the raw experimental data with a model theoretical signal. The procedure avoids any filtering of the data and allows a statistical analysis of the results. The theoretical signal is calculated ab initio and contains the relevant two-body $\gamma^{(2)}$, three-body $\gamma^{(3)}$, and four-body[30] $\gamma^{(4)}$ multiple scattering terms. In this contribution, only one two-body $\gamma^{(2)}$ term has been included in the fitting procedure, and it is due to the Cu−O first-shell interaction. The two-body terms are associated with pairs of atoms and probe their distances and variances. Data analysis is performed by minimizing a χ^2-like function that compares the theoretical model to the experimental signal.

The phase shifts for the photoabsorber and backscatterer atoms were calculated ab initio starting from the structural model that was presented in ref 6. They were calculated according to the muffin-tin approximation. The Hedin−Lundqvist complex potential[31] was used for the exchange-correlation potential of the excited state. Hereafter in the analysis, the starting signals have been successively recalculated to account for any important structural variation from the starting model. In fact, when a deviation of more than 10% of a selected structural parameter (e.g., atomic distance or angle) occurred with respect to the crystallographic values, the corresponding theoretical signal has been recalculated before being used in the fitting procedure. The core hole lifetime, Γ_c, was fixed to the tabulated value[32] and included in the phase shift calculation. The experimental resolution used in the fitting analysis was about 2 eV, in agreement with the stated value for the beamline used. The value of S_0^2 has been found to be 0.99. The relevant E_0 value are found to be displaced by several electronvolts with respect to the edge inflection point. In order to evaluate the effect of the structural disorder, the simulation was done by considering a non-Gaussian type of pair distribution functions. The γ-like (Γ) distribution has been used here[33] and proven to be very useful in previous studied systems.[26,34] The function depends on four parameters: the average bond distance, the bond variance, and the asymmetry coefficient (skewness) β defined as K_3/σ^3 where K_3 is the third cumulant of the distribution.

Spectral Data Treatment. In this section, $\mathbf{X}_{S,W}$ is the matrix of experimentally acquired measurements with S rows (number of acquired spectra) and W columns (number of points, i.e., energies, in each spectrum).

In a spectroscopic experiment as well as in XAS spectroscopy, the experimental matrix can be written as the product of a concentration and a spectrum matrix of pure compounds as follows

$$\mathbf{X}_{S,W} = \mathbf{C}_{S,F}\mathbf{A}_{F,W} \quad (1)$$

where $\mathbf{C}_{S,F}$ stands for the column matrix of the concentration profile of the F pure species and $\mathbf{A}_{F,W}$ is the row matrix of the XANES spectra of pure species.

The F significant factors (number of species) can be established, by EFA, as the ones emerging from a pool of noise factors fixed by a threshold level under which the factors are assumed as representing the noise. The matrix $\mathbf{C}^a_{S,F}$ stores the rank evolution received by the minimum of the forward and backward logarithm of the eigenvalues.[20]

If a closure condition is applicable, the $\mathbf{C}^a_{S,F}$ matrix can be used as a first guess of the concentration profile of the species after normalization over columns.

$$c_{s,f} = \frac{c_{s,f}}{\sum_{j=1}^{F} c_{s,j}} \quad (2)$$

It is noteworthy that the main information obtained from this calculation is the number of species and their range of existence. Similar information can be obtained by applying FSWEFA, a faster algorithm that calculates the local rank of the matrix by PCA on a window (of size N) moving through the matrix rows (in this work). The output of the FSWEFA is represented as a graph of the log transform of the eigenvalues versus the evolution parameter. The obtained curves are peak-shaped; the peaks are located at the equivalence point of two superimposing species. This means that we can use the peak position as a first approximation of the boundary point between the range of existence of different species. In this hypothesis, one species exists before the peak and another one after it.

FSWEFA gives us no idea of the concentration of the species, but it is very efficient in discovering low level species as peaks emerge from a flat noise background. The values of each column of the first guess concentration profile $\mathbf{C}^a_{S,F}$ matrix, necessary to initialize the iterative calculation, is set to 1 in the range of existence (limited by a peak) of the corresponding species and to 0 away from it. At the beginning, we hypothesize a disjointed existence of species, i.e., in the range where a species is defined and no other can exist. While in EFA the cutoff level for noise is a critical choice to identify the range of existence of the species, in FSWEFA the critical parameter is the dimensionality of the window (*N*) in which the optimum value has to be found by comparing several trials.

An initialization profile matrix is now available. It can be normalized as shown in eq 2 assuming the validity of the closure conditions. In our case we applied the additional constraints of non-negativity both of concentration and absorbance values. When negative values happen, they are set to 0 both in the concentration ($\mathbf{C}_{S,F}$) and spectra ($\mathbf{A}_{F,W}$) matrix. Then eq 1 can be used to alternatively calculate, by the least-squares method, the spectra matrix $\mathbf{A}_{F,W}$ and then, after constraints application, the concentration profiles $\mathbf{C}_{S,F}$. The iterative calculation stops when the residuals no longer vary with respect to those computed in the preceding cycle; details of our implementation of the algorithm are described in our previous work on spectroelectrochemistry.[24] In this article, both EFA and FSWEFA were checked as

(28) Filipponi, A.; Di Cicco, A.; Natoli, C. R. *Phys. Rev. B* **1995**, *52*, 15122.
(29) Filipponi, A.; Di Cicco, A. *Phys. Rev. B* **1995**, *52*, 15135.
(30) Giorgetti, M.; Berrettoni, M.; Filipponi, A.; Kulesza, P. J.; Marassi, R. *Chem. Phys. Lett.* **1997**, *275*, 108.
(31) Hedin, L.; Lundvquist, B. I. *J. Phys. C* **1971**, *4*, 2064.
(32) Krause, M.; Oliver, J. H. *J. Phys. Chem. Ref. Data* **1979**, *8*, 329.
(33) Filipponi, A. *J. Phys.: Condens. Matter* **1994**, *6*, 8415.
(34) D'Angelo, P.; Di Nola, A.; Filipponi, A.; Pavel, N. V.; Roccatano, D. *J. Chem. Phys.* **1994**, *100*, 985.

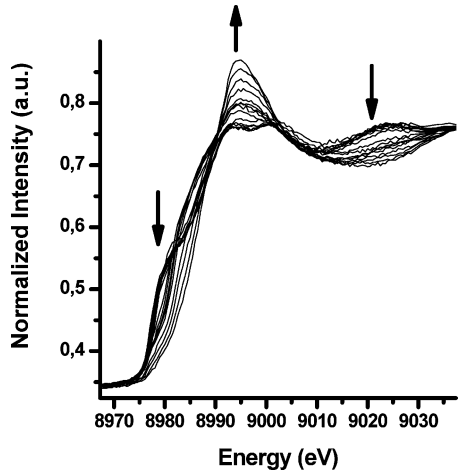

Figure 1. XANES spectra, taken at the Cu K-edge, recorded in sequence during the cell charging, i.e., during the lithium releasing process from the $Cu_{0.1}V_2O_5$ xerogel cathode. Arrows in the figure indicate the evolution of features during the experiment, from the 1st to the 53rd registered spectrum.

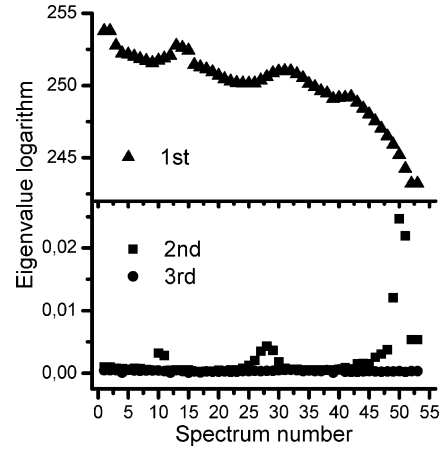

Figure 2. Graph of the eigenvalue logarithm versus the central point of the FSWEFA window. The graph is split to account for the large difference in their absolute value.

initialization methods, but as they give similar results and the second is faster we used only FSWEFA for the detailed analysis of the data.

RESULTS AND DISCUSSION

Figure 1 shows the series of XANES spectra, taken at the Cu K-edge, recorded in sequence during the cell charging, i.e., during the lithium releasing process. The evolution of the spectra upon the release of lithium is indicated by the arrows. From the raw data presented in the figure, it is interesting to note that the background profile, due to the "atomic" absorption and to the absorption by the electrochemical cell, is similar for all of the recorded spectra. As we already pointed out,[10] this behavior indicated that there were no secondary processes (such as dissolution of cathodic material or electrolyte leakage) during the electrochemical cycles, and thus the observed changes of the XANES spectra can be ascribed to structural and electronic modifications only. Hence, the condition (eq 2) could be applied, making a chemometric approach feasible to study the dynamics of the process as the closure condition is experimentally verified.

$$\sum_{j=1}^{F} c_{s,j} = \text{constant}$$

Figure 2 shows the log plot of the eigenvalues of three components versus the spectrum number. Because of the large magnitude difference of its value, the first eigenvalue is plotted separately from the second and third ones. Data were obtained with a three points FSWEFA. The use of a narrow window allows one to investigate completely the sequence with the uncertainty of one spectrum. Figure 2 shows three peaks on the plot of the second eigenvalue, so that up to four species could be present if we hypothesize the unimodality of each species. Analyzing the third eigenvalue it is clear that three species never exist at the same time as it never rises from the noise. The second eigenvalue enhancement indicates that two species exist at the same time, in which equivalent concentrations are expected at spectra 11, 28, and 50. The peak at spectrum11 is not significantly different from the noise and small compared to the other. To investigate in depth the actual number of the species, we have compared the results of the data treatment with the experimental evidence, and several trials were done (see the Supporting Information, Figures S1−S4). In a first attempt, we have hypothesized four nonsuperimposing species, and the optimizing algorithm has converged to three species only. Also, further testing over three species had the better results without considering the peak at spectrum 11. Hence, we believe that the peak at spectrum 11 was a fake one, and thus the successive data treatment has been done considering three species. The appearance of the peak in position 11 is due to the narrowness of the window we used that could interpret noise or a spike in the spectra as new species. As half of the window points are lost at the beginning and the other half at the end of the spectra treatment, we choose a narrow window that permits us to analyze the whole spectra accepting the risk to get a fake local rank.

Figure 3 shows the concentration profiles (Figure 3a) and the corresponding pure spectra (Figure 3b) obtained with the FSWEFA data treatment. The concentration profiles, depicted in Figure 3a, indicate the presence of three well-defined species with the corresponding range of existence. The first species, which has been identified in the previous paper,[3] is metallic Cu and it is the predominant one until spectrum 26, which corresponds to about 2.8 V of cell potential. A second, short living species is clearly predominant in the 30−47 range of recorded spectra, which corresponds to 3.0−3.3 V. Finally, a third species appears after spectrum 42 (3.75 V) and becomes predominant after spectrum 49. Scans from 40 to 50 reflect a transition from species 2 to species 3, whose structure has been previously identified as well.[3] This corresponds to a CuO_4 quasi planar figure with the copper interacting with the apical oxygen of a V_2O_5 double-sheet. Further, the local coordination environment of the "new" detected species 2 could be identified by EXAFS analysis, by using one of the EXAFS spectrum in the 32−40 range of recorded spectra, because, in them, the single chemical phase is certain. This has been done, and Figure 4 presents the EXAFS best fit results for the 36th spectrum. Panel a shows the comparison of the experimental and theoretical EXAFS signal, whereas the corresponding Fourier transform (FT) is indicated

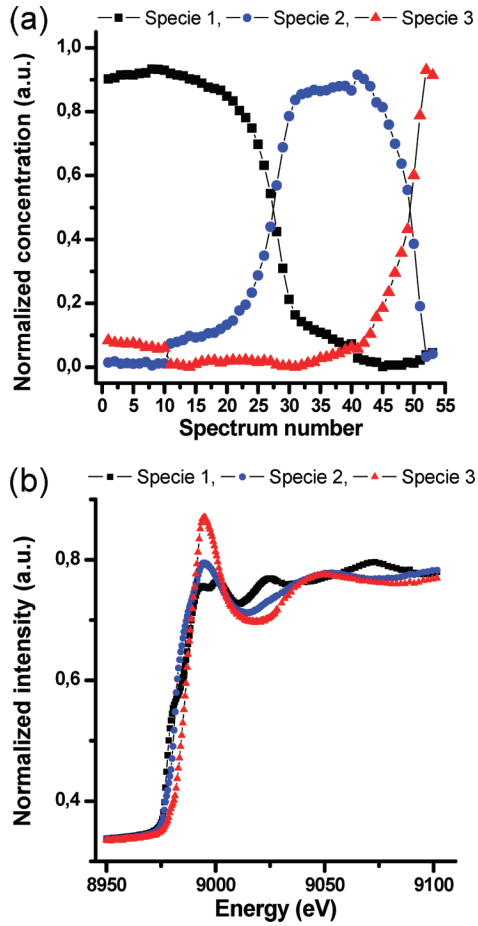

Figure 3. Computed concentration profiles (a) obtained with the MCR data treatment described in the article and the corresponding pure spectra (b).

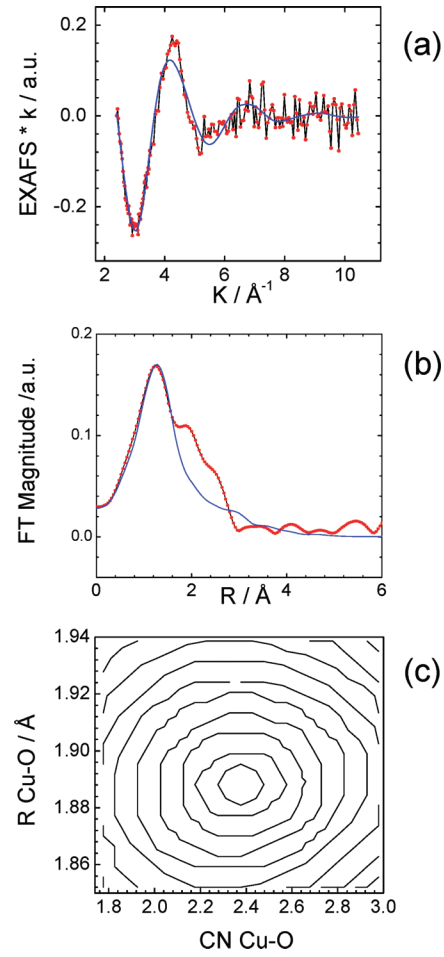

Figure 4. EXAFS fitting analysis of the experimental spectrum 36. (a) Comparison of the experimental (*) and theoretical (—) k-extracted EXAFS taken at the Cu K-edge. (b) Comparison of the experimental (*) and theoretical (—) Fourier transform of the k-extracted EXAFS taken at the Cu K-edge. The first shell contribution is well determined by the fitting analysis. (c) Two-dimensional section of the parameter space (contour plots) for the relevant parameters Cu−O distance and their corresponding coordination number (CN). The inner elliptical contour corresponds to the 95% confidence level.

in panel b. Panel a of Figure 4 reveals a good agreement between the theoretical curve and the experimental one, even though the fit has been done considering a very limited number of parameters. This indicates the reliability of the proposed Cu site and the accuracy of the data analysis. Briefly, only one two-atom contribution has been included in the fitting procedure: $\gamma^{(2)}$ Cu−O (first shell) with its coordination number was allowed to float. Also, panel b of Figure 4 is evidence that this first shell contribution is well determined by the fitting analysis. The overall number of parameters included in the fitting procedure was seven: four are related to the structural terms describing the Cu−O first shell, one bond distance and its coordination number, one asymmetry coefficient β, one EXAFS Debye−Waller factor, and three nonstructural terms: E_0, S_0^2, and the experimental resolution.

Hence, this simple structural analysis on the spectrum 36 indicated a close Cu−O interaction at about 1.89(2) Å with a coordination number of 2.4(4). Structurally speaking, the model for species 2 is a CuO_2 figure with the copper interacting with two oxygen of the V_2O_5 double sheets. Also, an EXAFS Debye−Waller factor of 0.019(4) and $\beta = 0.7(2)$ is observed. The large displacement from the Gaussian value for the distribution functions (asymmetry) is due to the large structural disorder that, of course, is typically present in insertion materials. The numbers in parentheses indicate the associated statistical errors. They were determined by the correlation maps (contour plot[35]) for each pair of highly correlated parameters. Panel c of Figure 4 shows the contour plot for the most important parameters, the Cu−O distance and their corresponding coordination number (CN). The inner elliptical contour corresponds to the 95% confidence level. The present EXAFS analysis indicates that the copper local atomic environment in "species 2" is different from those of the fully charged (CuO_4) and fully discharged cathode (metallic Cu). To exclude unambiguously the occurrence, for the spectrum 36, of a CuO_4 or metal Cu structural model, Figures 5 and 6 display an EXAFS analysis of spectrum 36 where the experimental signal has been tested with these two structure. As seen from the higher intensity of the residual curve in both cases, the two fitting analysis have failed. This evidences once again the occurrence of a different chemical environment for "species 2" with respect to "species 1" and "species 3", which has been identified by chemometry.

From Figure 3a, it is evident that there is a subrange of exclusive existence for each specie in the range of investigation.

(35) Filipponi, A. *J. Phys.: Condens. Matter* **1995**, *7*, 9343.

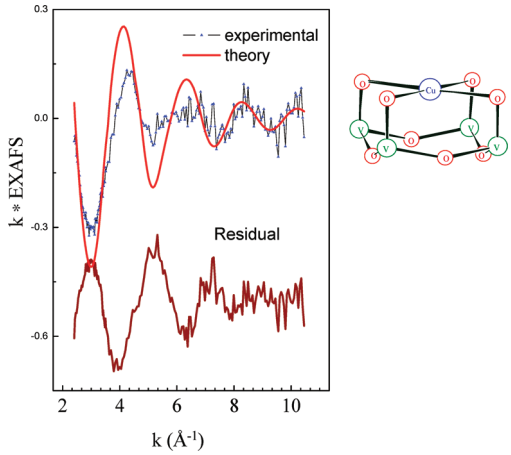

Figure 5. EXAFS fitting analysis of spectrum 36 considering the structural model of "specie 3" (Cu is 4-fold coordinated by 4 apical oxygen of a V_2O_5 sheet: CuO_4 model). Comparison of the experimental (*) and theoretical (—) k-extracted EXAFS taken at the Cu K-edge of the $Cu_{0.1}V_2O_5$ XRG material. The CuO_4 sites are indicated at the right and occurs when the cathode is completely charged (from ref 10). The fitting procedure clearly indicates a large residual signal, thus testifying a different Cu local site for spectrum 36.

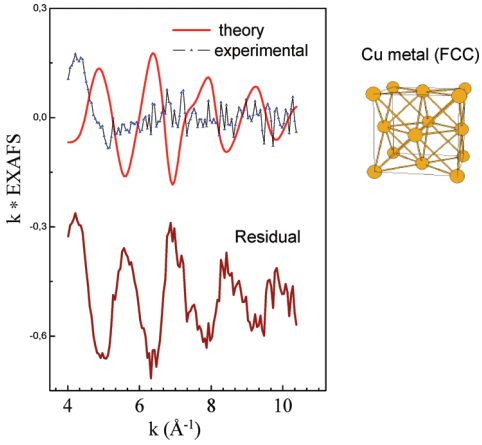

Figure 6. EXAFS fitting analysis of spectrum 36 considering the structural model of "species 1" (Cu has a typical face-centered cubic (fcc) structure). Comparison of the experimental (*) and theoretical (—) k-extracted EXAFS taken at the Cu K-edge of the $Cu_{0.1}V_2O_5$ XRG material using an fcc structure. The fcc structure is indicated at the right and occurs when the cathode is completely discharged (from ref 10). The fitting procedure clearly indicates a large residual signal, thus testifying a different Cu local site for spectrum 36.

The conversion of species 1 to species 3 takes place gradually by a subsequent two step process. Consequently, when the relative concentration of two species is identical, a condition corresponding to the crossing point of the concentration profile (for instance at spectra 28 and 52), an isosbestic point should be observable in the experimental spectra. This is confirmed in Figure 5 which shows the experimental spectra from spectra 1 to 35 (Figure 7a) and from spectra 36 to 53 (Figure 7b). It is evident one isosbestic point at 8982 eV, marked with a circle in Figure 7a, due to species 1 and 2, whereas two well-defined isosbestic point at 8990 and 9004 eV, are visible in Figure 7b. They arise, respectively, from the various spectra of species 2 and 3.

To gain a more complete understanding, the comparison of the three pure spectra as obtained from the MCR analysis

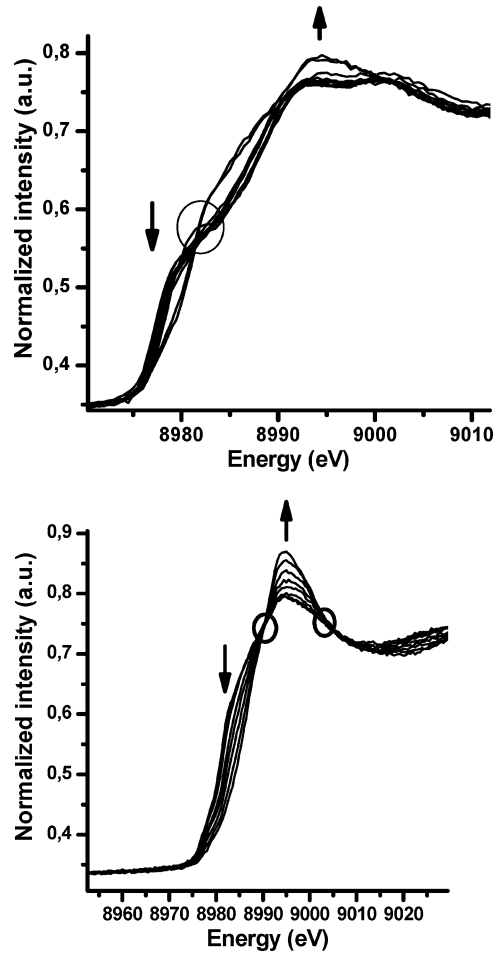

Figure 7. Selected experimental spectra showing the presence of well-defined isosbestic points during phase changing. The selections were chosen as suggested by Figure 3a. Upper: species 1 to species 2 conversion (scans 1, 3, 5, 8, 11, 14, 17, 21, 25, 30, 34). Bottom: species 2 to species 3 conversion (scans 34, 37, 40, 43, 47, 49, 50, 51, 52, 53).

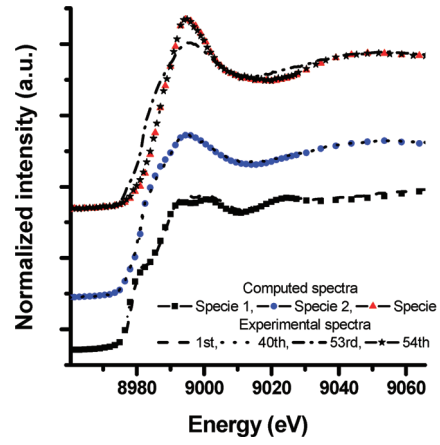

Figure 8. Comparison of computed spectra with the experimental ones. The experimental signals are well reproduced in the calculated pure spectra, except for species 3, which is obtained experimentally after a cell rest period. The spectra in the *y* direction are offset for the sake of clarity.

(shown in Figure 3b) to some selected experimental ones is indicated in Figure 8. The experimental spectra were chosen after examination of Figure 3a and can be summarized as follows: spectrum 1 for "species 1", spectrum 40 for "specie

2", and spectrum 53 for "specie 3". From Figure 8 it is clear that the experimental signals match quite well with the calculated pure component signals obtained from the chemometric approach. This underlines the capability of the present chemometric analysis to study dynamic XANES spectra. The only mismatch appears while considering spectrum 53 (end of battery charging), which is more similar to the "species 2" one. However, a very good agreement is obtained by comparing "species 3" to spectrum 54, which has been obtained after a rest period. Because no current flows during the rest period, the good match between "species 3" to spectrum 54 instead of spectrum 53 reveals a small hysteresis of the cell behavior. This is mainly due to uncompensated IR drop and a kinetic issue; i.e., the cell composition modification and the subsequent structure rearrangement around Cu are not as fast as the imposed current would require.

CONCLUSIONS

A chemometric approach has been applied to a well-defined set of experimental XAS data recorded in situ, allowing a more complete understanding of the cell dynamic. Among some different chemometric techniques, the application of the MCR to the studied $Cu_{0.1}V_2O_5$/Li ions battery has revealed the existence range of the various species involved during the experiment. Because no secondary processes are involved in our experiment, the closure condition (eq 2) can be applied. An iterative refinement permits optimization of the concentration profiles, whose values are hypothesized by the FSWEFA ranges, and computation of the pure spectra. The pure spectra have been obtained and compared to the experimental ones, with very good agreement. The proposed data treatment evidenced, for the first time, the occurrence of three species during the charging of the $Cu_{0.1}V_2O_5$ xerogel/Li ions battery. This information, even though suggested by the CV curve of the analyzed cathode,[36] was never confirmed before. The EXAFS analysis confirms the different chemical environment of species 2 with respect to those of species 1 and 2.

More generally, this article shows the potentiality of the joined chemometric-dynamic XAS approach to study the local structural dynamics of atomic species (Cu in this case) which undergo some structural modifications. In particular, the chemometric approach permits a quicker data interpretation that would be very time-consuming and very challenging if a mixed phase could have been present and if only EXAFS was relied on.

ACKNOWLEDGMENT

Measurements at Brookhaven National Laboratory were supported by the DOE under Contract DE-FG02-01ER15221. We also thank the University of Bologna for RFO funding.

SUPPORTING INFORMATION AVAILABLE

EFA-MRC and FSWEFA-MRC analysis using three and four species and some contour plots of the EXAFS fitting analysis for spectrum 36. This material is available free of charge via the Internet at http://pubs.acs.org.

Received for review December 16, 2009. Accepted March 22, 2010.

AC902865H

(36) Coustier, F.; Hill, J.; Owens, B. B.; Passerini, S.; Smyrl, W. H. *J. Electrochem. Soc.* **1999**, *146*, 1355.